REPORT DOCUMENTATION PAGE

Form Approved
OMB No. 0704-0188

1. AGENCY USE ONLY (Leave blank)	2. REPORT DATE	3. REPORT TYPE AND DATES COVERED
	1990, Sept. 5	Technical Report #4 10/89-9/90

TITLE AND SUBTITLE
UNCLASSIFIED: On the Crystal Structure of $KInS_2$-I

5. FUNDING NUMBERS
N00014-90WX24148

AUTHOR(S)
C. K. Lowe-Ma, D. O. Kipp, and T. A. Vanderah

PERFORMING ORGANIZATION NAME(S) AND ADDRESS(ES)
Research Department
Naval Weapons Center
Chemistry Division Code 3850
Naval Weapons Center
China Lake, CA 93555

8. PERFORMING ORGANIZATION REPORT NUMBER

9. SPONSORING/MONITORING AGENCY NAME(S) AND ADDRESS(ES)
Office of Naval Research
Chemistry Program
800 N. Quincy St.
Arlington, VA 22217

10. SPONSORING/MONITORING AGENCY REPORT NUMBER

11. SUPPLEMENTARY NOTES
Submitted for publication in Journal of Solid State Chemistry

12a. DISTRIBUTION/AVAILABILITY STATEMENT

DISTRIBUTION STATEMENT A
Approved for public release;
Distribution Unlimited

12b. DISTRIBUTION CODE

13. ABSTRACT (Maximum 200 words)

$KInS_2$-I, the ambient-pressure form of this composition, crystallizes in monoclinic space group $C2/c$; a = 10.981(3), b = 10.979(3), c = 15.010(5) Å, β = 100.55(2)°, Vol = 1779.2(9) Å^3, Z = 16, D_x = 3.257 g/cm^3 for M_F = 218.04. An X-ray single-crystal structure determination has confirmed that $KInS_2$-I has the $TlGaSe_2$ structure. The bonding in $KInS_2$-I is highly covalent and exhibits both two-dimensional and three-dimensional features. The structure is comprised of layers of vertex-sharing $[In_4S_{10}]$ adamantane-like units built of $[InS_4]$ tetrahedra. The stacking arrangement of these layers creates channels that contain the potassium ions in distorted trigonal prismatic sites that provide the three-dimensionality of the structure. The covalent nature of the interlayer potassium-sulfur bonding is reflected in the non-micaceous morphology and water-stability of the transparent light-yellow crystals.

14. SUBJECT TERMS
ternary indium sulfides, crystal structure

15. NUMBER OF PAGES

16. PRICE CODE

17. SECURITY CLASSIFICATION OF REPORT	18. SECURITY CLASSIFICATION OF THIS PAGE	19. SECURITY CLASSIFICATION OF ABSTRACT	20. LIMITATION OF ABSTRACT
Unclassified	Unclassified	Unclassified	Unlimited

OFFICE OF NAVAL RESEARCH

Grant or Contract N00014-90WX24148

R&T Code 4134046

Technical Report No. 4

On the Crystal Structure of $KInS_2$-I

by

C. K. Lowe-Ma, D. O. Kipp, T. A. Vanderah

Submitted for publication
in
Journal of Solid State Chemistry

Chemistry Division
Research Department
Naval Weapons Center
China Lake, CA 93555

August 1990

On the Crystal Structure of $KInS_2$-I

C. K. Lowe-Ma, D. O. Kipp, T. A. Vanderah
Chemistry Division, Research Department
Naval Weapons Center, China Lake, CA 93555

ABSTRACT

$KInS_2$-I, the ambient-pressure form of this composition, crystallizes in monoclinic space group *C2/c*; a = 10.981(3), b = 10.979(3), c = 15.010(5) Å, β = 100.55(2)°, Vol = 1779.2(9) $Å^3$, Z = 16, D_x = 3.257 g/cm^3 for M_F = 218.04. An X-ray single-crystal structure determination has confirmed that $KInS_2$-I has the $TlGaSe_2$ structure. The bonding in $KInS_2$-I is highly covalent and exhibits both two-dimensional and three-dimensional features. The structure is comprised of layers of vertex-sharing $[In_4S_{10}]$ adamantane-like units built of $[InS_4]$ tetrahedra. The stacking arrangement of these layers creates channels that contain the potassium ions in distorted trigonal prismatic sites that provide the three-dimensionality of the structure. The covalent nature of the interlayer potassium-sulfur bonding is reflected in the non-micaceous morphology and water-stability of the transparent light-yellow crystals.

INTRODUCTION

Our investigation of ternary indium sulfide systems was undertaken to identify new compounds for possible applications as optical ceramics and to confirm reported structures and structural interrelationships. In a series of crystal growth experiments using eutectic halide fluxes [1], large numbers of high-quality platelets and rods of the compound $KInS_2$ were obtained. We became interested in the polymorphism reported for this composition and the related coordinative versatility of trivalent indium, namely, tetrahedral versus octahedral. This coordinative versatility plays a significant role in determining infrared optical properties.

Three polymorphs of $KInS_2$ have been previously identified - one ambient-pressure form ($KInS_2$-I) [2] and two high-pressure forms ($KInS_2$-II and -III) [3]. Although, to our knowledge, full single-crystal structure determinations have not been reported for any of the polymorphs, possible structures have been deduced from studies of polycrystalline samples. $KInS_2$-I is reportedly isostructural with ambient-pressure $RbInS_2$-I and $TlGaSe_2$ [2, 4] and crystallizes with monoclinic lattice symmetry (a = 15.64, b = 10.88, c = 11.16 Å; β = 103°) [2]; this structure-type features tetrahedral coordination of the trivalent cations while the larger monovalent ions occupy trigonal prisms [5]. $KInS_2$-I transforms to two other higher-density polymorphs at elevated pressures and temperatures. $KInS_2$-II (30 kbar, 1000°C) [3] is isostructural with TlSe ($Tl^{I}Tl^{III}Se_2$) with a tetragonal unit cell (I4/mcm; a = 7.769(3), c = 6.672(3) Å) [3] and features chains of opposite-edge-shared [InS_4] tetrahedra and eight-coordinate potassium in square anti-prismatic sites. $KInS_2$-III (20 kbar, 350°C) [3] exhibits the α-$NaFeO_2$ structure with a hexagonal unit cell (a = 3.875(2), c = 21.794(5) Å) [3]. This structure is an ordered rock salt derivative; the coordination of both potassium and indium is octahedral with the two metals segregated on alternate (111) planes of the parent NaCl structure. $KInS_2$-II can be converted to $KInS_3$-III, the highest-density phase, by application of 40 kbar pressure at 1000°C. Both high-pressure forms convert to $KInS_2$-I at ambient pressure above 300°C.

Limited information on the physical properties of the $KInS_2$ phases is available. $KInS_2$-I melts at 1024°C in vacuo and is stable in air below 380°C [6]. A band-gap of 3.0 eV was found for crystals of $KInS_2$-I [7]. The infrared spectrum of $KInS_2$-I measured below 400 cm^{-1} indicated groups of absorption bands in the regions 350-290, 180-110, and below 100 cm^{-1} [6].

In the present study, a full X-ray single-crystal structure determination was carried out for $KInS_2$-I to elucidate structural details and confirm its relationship to the $TlGaSe_2$ structure [5].

EXPERIMENTAL

In previous studies, $KInS_2$-I was prepared as crystals from melts of S, K_2CO_3, and In_2O_3 [2, 6] or S, K, and In_2S_3 [5] at 800-1000°C and in powder form from $KInO_2$ or K_2CO_3 and In_2O_3 under H_2S at 600-800°C [6]. In the present study, crystals of $KInS_2$-I were grown from KCl-containing eutectic halide fluxes as a co-product of crystallization of compounds in the Ca-In-S and Sr-In-S systems [1]. The very pale yellow-orange square platelets and rectangular rods of $KInS_2$-I had well-formed faces and were easily separated from the smaller whiskers of the alkaline-earth indium sulfides under a microscope. Semi-quantitative elemental analyses were obtained with a scanning electron microscope by energy-dispersive X-ray spectroscopy (EDX) using an AMRAY 1400, TRACOR TN2000 analyzer. The results of multiple determinations were consistent with the stoichiometry $KInS_2$ for both the platelets and the rods; no incorporation of Ca, Sr, or Cl was detected in any of the crystals.

Unit cell parameters were obtained with a Nicolet R3 single-crystal diffractometer using monochromated Mo Kα. Unit cells were determined for two platelets [platelet 1: a = 10.978(3), b = 10.984(3), c = 15.015(5) Å, β = 100.53(3)°; platelet 2: a = 10.981(3), b = 10.979(3), c = 15.010(5) Å, β = 100.55(2)°] and a rod [a = 10.975(6), b = 10.999(7), c = 15.030(10) Å, β = 100.63(5)°]. The platelets and rod were all found to be C-centered monoclinic. These results are consistent with those reported previously for $KInS_2$-I [2]. Intensity data were obtained for pale yellow-orange platelet 2, approximate dimensions 0.02 x 0.11 x 0.24 mm, with a Nicolet R3 using monochromated Mo Kα at 293 K; 25 computer-centered reflections were used for the symmetry-constrained least-squares determination of the unit cell. Parameters for intensity data collection parameters were as follows: $2\theta/\theta$ scans; 4° - 12°/min variable scan speed; scan width of 2.0° plus Kα separation; ratio of total background to total scan time of 1.0; 2θ range of 4° to 60° (λ = 0.71073 Å); indices ranged from $-16 \le h \le 16$, $0 \le k \le 16$, $-22 \le l \le 22$ with $h+k=2n+1$ not collected; 3 check reflections, (0,8,0), (0,0,10), (4,4,-1), collected every 93 reflections with most variations less than 3%. The data were corrected for Lorentz and polarization

effects and, based on ψ - scans of 22 reflections, were empirically corrected for absorption assuming a lamellar model (minimum transmission of 0.52; maximum transmission of 0.95). Reflections with h0*l*, h=2n+1 and *l*=2n+1, and 00*l*, *l*=2n+1 were absent indicating space groups *Cc* or *C2/c*. In *C2/c*, R_{merge} = 0.035 for 2962 unique reflections; 1970 with $|F_o| \geq 3\sigma(F)$ were considered observed and used for structure solution and refinement.

Initial indium and sulfur atomic positions were obtained by Patterson methods followed by direct methods phase expansion. Remaining sulfur and potassium positions were obtained by Fourier cycling. After full-matrix least-squares minimization of $\Sigma w(F_o - kF_c)^2$ using neutral-atom scattering factors, R = 0.047 with anisotropic thermal parameters; at this point significant difference Fourier peaks were observed. The two strongest difference peaks were modeled as partially-occupied indium sites based on the sulfur - unknown peak bond lengths. Additional weak difference peaks were also observed near the two sulfur atoms S(2) and S(5), near K(2), and near both indium atoms In(1) and In(2), although additional atoms at these difference peak positions were not refined. For 82 parameters, including two partially-occupied (disordered) indium sites, full-matrix least-squares refinement, with weighting $w = 1/[\sigma^2(F) + 0.0008F^2]$, converged; for the final cycle, the largest and mean shift/esd ratios were 0.24 and 0.02 respectively with R = 0.035, wR = 0.044, GOF = 1.04. All calculations were accomplished using SHELXTL PC™ package of programs [8]. Final atomic coordinates and thermal parameters are given in Table I.[1]

---

1. See NAPS document No. ____ for ___ pages of supplementary material. Order from ASIS/NAPS, Microfiche Publications, P.O. Box 3513, Grand Station, New York, NY 10163. Remit in advance $4.00 for microfiche copy or for photocopy, $7.75 up to 20 pages plus $.30 for each additional page. All orders must be prepaid. Institutions and Organizations may order by purchase order. However, there is a billing and handling charge for this service of $15. Foreign orders add $4.50 for postage and handling, for the first 20 pages, and $1.00 for additional 10 pages of materials, $1.50 for postage of any microfiche orders.

RESULTS

$KInS_2$-I is isostructural with $TlGaSe_2$ [5] and exhibits features of both a two-dimensional and three-dimensional structure. The structure consists of layers of vertex-sharing $[In_4S_{10}]$ adamantane-like units that are structurally analogous to vapor-phase P_4O_{10}; each $[In_4S_{10}]$ unit is comprised of four vertex-sharing $[InS_4]$ tetrahedra surrounding an empty octahedral site. One $[In_4S_{10}]$ unit is illustrated in Figure 1 both as a ball-and-stick representation with thermal ellipsoids and as a polyhedral representation. The In-S connections within one layer of $[In_4S_{10}]$ units are illustrated in Figure 2. Vertex-sharing of the $[In_4S_{10}]$ units creates channels perpendicular to one another in the ab-plane that contain the potassium atoms. The layers of vertex-sharing $[In_4S_{10}]$ units stack perpendicular to c^* and each layer is related to the ones above and below by a 2-fold rotation in the plane of a layer. The edges of the large $[In_4S_{10}]$ units in one layer nestle into the channels of the layers above and below as shown in Figure 3, thus completing the trigonal prismatic coordination spheres about the potassiums.

As shown in Figure 4(a,b), each potassium is surrounded by six sulfurs in a distorted trigonal prism. The two crystallographically distinct potassiums alternate along each channel in trigonal prisms that share triangular faces. Polyhedral linkage of the trigonal prisms about K(1) and K(2) to those in the other channels differ, but have similar sets of two shorter (3.174 to 3.194 Å) plus four longer (3.274 to 3.422 Å) distances to sulfur. Two additional sulfurs are located at 3.977 - 3.997 Å, distances considerably shorter than the sum of the van der Waals radii, 4.55 Å [9], but slightly longer than metal-metal distances to nearby potassium and indium atoms (Table II). The two shortest potassium-sulfur distances occur from a potassium in the channel of one layer to sulfurs S(2) and S(5) along the edge of an adjoining layer, thus imparting strong three-dimensional character to the structure. Coordination involving the sulfur atoms in the middle of the layers of $[In_4S_{10}]$ units, S(1), S(3), and S(4), result in potassium-sulfur distances averaging 3.34(5) Å. The K-S bond distances observed in $KInS_2$ are consistent with those observed in other solids: 3.20 Å in K_2S (tetrahedral coordination) [10], 3.275 to 3.361 Å in KIn_5S_8 (approximately trigonal prismatic with two additional sulfurs at 3.776 Å) [11], and 3.32 to 3.50 Å in $KFeS_2$ (distorted eight-coordination) [12].

The In-S distances within the two crystallographically distinct $[InS_4]$ tetrahedra (Table II) range from 2.421 to 2.482(3) Å with a mean value of 2.45(2) Å, and are

consistent with the mean distances observed in other compounds containing tetrahedral InS_4 groups; e.g., 2.46 Å in β-In_2S_3 [13], 2.50 Å in KIn_5S_8 [11], 2.45 Å in $LiInS_2$ [7], 2.48 Å in $AgInS_2$ [14], 2.48 Å in $Mg_{0.83}In_{2.113}S_4$ [15], and 2.47 Å in $BaIn_2S_4$ [16]. The S-In-S bond angles in $KInS_2$ are slightly distorted from the ideal and range from 105.1 to 113.3(1)°.

The structure contains five crystallographic types of sulfur atoms divided into two structurally similar sets. Half of the sulfur atoms occupy the S(2) and S(5) positions that comprise the string of tetrahedral edges that projects into the potassium channels (see Figure 4); each of these sulfurs is four-coordinate by two indiums plus two potassiums arranged in a distorted square plane. The other half of the sulfurs occupy the S(1), S(3), and S(4) sites in the middle of the layers of $[In_4S_{10}]$ units and are irregularly six-coordinate by two indium plus four potassium atoms.

Two significant peaks in the difference Fourier map were modeled and refined as partially-occupied indium sites; these sites are translated from positions of In(1) and In(2) by x=0.5. Additional peaks observed in the difference map could arise from other atoms undergoing a similar translation. The slight disorder among indium sites obtained in our refinement may be related to the two stacking arrangements that are possible for the layers of the $[In_4S_{10}]$ units. The second layer can be translated along the (110) direction (the direction of the potassium chains) by one S-S distance without changing the local coordination environment of any of the atoms. This type of stacking disorder was elegantly described for HgI_2 [17], and was also reported for $TlGaSe_2$ [5].

DISCUSSION

$TlGaSe_2$ was originally reported in space group *Cc* [5]; subsequent work indicated that the structure is more correctly described in space group *C2/c* [18, 19] with transformed atomic coordinates [18] very similar to those obtained for $KInS_2$-I in the present study. Other compounds reported to be isostructural with $TlGaSe_2$ and $KInS_2$-I include $KInSe_2$ [19]; $RbInS_2$-I, $CsInS_2$, $KTlS_2$, $RbTlS_2$, and $CsTlS_2$ [2]; and $TlAlS_2$, $TlAlSe_2$, $TlGaS_2$, $TlInS_2$, and $RbGaS_2$ [4].

Although the $KInS_2$-I structure should be regarded as highly covalent, it does bear

some similarity to closest-packed-derived structures such as that of HgI_2 [17]. In the proposed structure for the unstable orange modification of HgI_2 [17], the iodine atoms occupy the positions of closest-packing (cp) in a cubic A-B-C sequence. One-fourth of each of the two types of tetrahedral interstices between the layers are equally occupied by the mercury atoms, resulting in layers of vertex-sharing $[Hg_4I_{10}]$ units that are structurally analogous to those comprised of $[In_4S_{10}]$ units in $KInS_2$-I. In the structure of $KInS_2$-I, the cp layers are highly distorted by the covalent nature of the bonding in such a way as to push the layers slightly apart and form the strings of face-sharing trigonal prisms that comprise the channels and accommodate the potassium atoms. A more open structure than that of HgI_2 results, leaving only domains of cubic closest-packing within the layers of $[In_4S_{10}]$ units.

The three-dimensional character of the structure is reflected in the relatively short K-S(2) and K-S(5) bond distances that serve to provide strong interlayer coupling; the $KInS_2$-I crystals are non-micaceous and occur as both square platelets and rectangular rods. Raman data obtained in a study of the isostructural compounds $TlGaS_2$, $TlGaSe_2$, and $TlInS_2$ [18] were interpreted as indicating a range of interatomic force constants that ruled out a simplified picture of strong intralayer vs. weak interlayer bonding.

CONCLUSIONS

A single-crystal structure structure determination of a pale yellow-orange platelet of $KInS_2$-I confirmed that this compound is isostructural with $TlGaSe_2$ [5]. The structure consists of layers of vertex-sharing $[In_4S_{10}]$ adamantane-like units that are analogous to vapor-phase P_4O_{10}. The stacking of the layers creates channels perpendicular to one another that contain potassium atoms in trigonal prismatic sites. Short interlayer K-S bonding imparts three-dimensionality to the solid.

ACKNOWLEDGMENTS

The authors wish to thank Bob Woolever for the SEM/EDX analyses. D.O.K.'s post-doctoral fellowship was administered by the American Society for Engineering Education. This work was supported by the Office of Naval Research.

REFERENCES

1. D.O. Kipp, C.K. Lowe-Ma, and T.A. Vanderah, *Chemistry of Materials*, in press.

2. H. Schubert and R. Hoppe, *Z. Naturforsch.* **25b**, 886 (1970).

3. K.-J. Range and G. Mahlberg, *Z. Naturforsch.* **30b**, 81 (1975).

4. D. Müller, F.E. Poltmann, and H. Hahn, *Z. Naturforsch.* **29b**, 117 (1974).

5. D. Müller and H. Hahn, Z. anorg. allg. Chem. **438**, 258 (1978).

6. S.K. Kovach, E.E. Semrad, Yu.V. Voroshilov, V.S. Gerasimenko, V.Yu. Slivka, and N.P. Stasyuk, *Inorg. Materials* **14**, 1693 (1978).

7. Z.Z. Kish, E.Yu. Peresh, V.B. Lazarev, and E.E. Semrad, *Inorg. Materials* **23**, 697 (1987).

8. SHELXTL PC™, Version 4.1, Siemens Analytical X-ray Instruments, (May 1990).

9. A. Bondi, *J. Phys. Chem.* **68**, 441 (1964).

10. R.W.G. Wyckoff, "Crystal Structures", 2nd edition, Vol. 1, Wiley Interscience: New York, p. 242 (1963).

11. D. Carré and M.P. Pardo, *Acta Cryst* **C39**, 822 (1983).

12. W. Bronger, *Z. anorg. allg. Chem.* **359**, 225 (1968).

13. G.A. Steigmann, H.H. Sutherland, and J. Goodyear, *Acta Cryst.* **19**, 967 (1965).

14. H. Hahn, G. Frank, W. Klingler, A.-D. Meyer, and G. Störger, *Z. anorg. allg. Chem.* **271**, 153 (1953).

15. B. Eisenmann, M. Jakowski, and H. Schäfer, *Mat. Res. Bull.* **19**, 77 (1984).

16. B. Eisenmann, M. Jakowski, W. Klee, and H. Schäfer, *Rev. Chim. minérale* **20**, 255 (1983).

17. D. Schwarzenbach, *Z. Kristallogr.* **128**, 97 (1969).

18. W. Henkel, H.D. Hochheimer, C. Carlone, A. Werner, S. Ves, and H.G. v.Schnering, *Phys. Rev. B* **26**, 3211 (1982).

19. B. Krebs, *Angew. Chem. Int. Ed. Engl.* **22**, 113 (1983).

Table I. Atomic Coordinates and Thermal Parameters ($Å^2$) for $KInS_2$-I

	x	y	z	U(eq)*
In(1)	0.39969(5)	-0.18817(6)	0.34473(5)	0.0144(1)
In(2)	0.14768(5)	0.06323(6)	0.34498(5)	0.0150(1)
K(1)	0.4663(2)	0.1875(2)	0.1162(1)	0.0343(5)
K(2)	0.2834(2)	0.4383(2)	0.3832(1)	0.0340(5)
S(1)	0.2591(2)	0.1927(3)	0.2506(1)	0.020(1)
S(2)	0.2983(2)	-0.0629(2)	0.4446(1)	0.033(1)
S(3)	0.5000	-0.0576(4)	0.2500	0.021(1)
S(4)	0.0 0	-0.0746(3)	0.2500	0.015(1)
S(5)	0.0490(2)	0.1876(2)	0.4461(1)	0.040(1)
In(3)	0.4046(14)	0.3148(16)	0.3453(13)	0.020
In(4)	0.3606(24)	0.0540(26)	0.1539(22)	0.020

* Equivalent isotropic U defined as one third of the trace of the orthogonalized U_{ij} tensor

	U_{11}#	U_{22}	U_{33}	U_{12}	U_{13}	U_{23}
In(1)	0.0139(2)	0.0144(2)	0.0151(2)	0.0031(1)	0.0036(1)	-0.0002(1)
In(2)	0.0140(2)	0.0150(2)	0.0158(2)	0.0033(1)	0.0024(1)	0.0005(1)
K(1)	0.0400(9)	0.0424(9)	0.0198(8)	-0.0232(8)	0.0034(6)	0.0004(6)
K(2)	0.0417(9)	0.0418(9)	0.0182(7)	0.0207(8)	0.0048(6)	0.0005(6)
S(1)	0.016(1)	0.015(1)	0.027(1)	-0.005(1)	0.005(1)	0.004(1)
S(2)	0.043(1)	0.045(1)	0.011(1)	0.033(1)	0.002(1)	0.000(1)
S(3)	0.019(1)	0.024(1)	0.022(1)	0.0	0.010(1)	0.0
S(4)	0.015(1)	0.006(1)	0.022(1)	0.0	0.000(1)	0.0
S(5)	0.050(1)	0.052(1)	0.017(1)	0.039(1)	0.004(1)	-0.001(1)

The form of the anisotropic thermal parameters are:

$$-2\pi^2(h^2a^{*2}U_{11} + \ldots + 2klb^*c^*U_{12})$$

Table II. Bond Lengths (Å) and Bond Angles (°)* in $KInS_2$-I.

In(1)-S(2)	2.448 (2)	In(2)-S(1)	2.482 (3)
In(1)-S(3)	2.421 (3)	In(2)-S(2)	2.447 (2)
In(1)-S(1)	2.426 (2)	In(2)-S(4)	2.471 (2)
In(1)-S(5)	2.439 (2)	In(2)-S(5)	2.438 (3)
In(1)-K(1)	4.006 (2)	In(2)-K(2)	4.010 (2)
In(1)-K(2)	3.894 (2)	In(2)-K(2)	3.891 (2)
K(1)-S(1)	3.305 (3)	K(2)-S(1)	3.334 (4)
K(1)-S(1)	3.299 (3)	K(2)-S(1)	3.422 (4)
K(1)-S(2)	3.188 (3)	K(2)-S(2)	3.194 (3)
K(1)-S(2)	3.992 (3)	K(2)-S(3)	3.378 (2)
K(1)-S(2)	3.977 (3)	K(2)-S(4)	3.379 (2)
K(1)-S(3)	3.337 (4)	K(2)-S(5)	3.183 (3)
K(1)-S(4)	3.274 (3)	K(2)-S(5)	3.997 (3)
K(1)-S(5)	3.174 (3)	K(2)-S(5)	3.986 (3)
K(1)-In(1)	4.006 (2)	K(2)-In(1)	3.894 (2)
K(1)-K(1)	3.948 (3)	K(2)-In(2)	4.010 (2)
K(1)-K(2)	3.890 (3)	K(2)-In(2)	3.891 (2)
K(1)-K(2)	3.874 (3)	K(2)-K(1)	3.890 (3)
		K(2)-K(1)	3.874 (3)
S(1)-In(1)	2.426 (2)	S(3)-In(1)	2.421 (3) x 2
S(1)-In(2)	2.482 (3)	S(3)-K(1)	3.337 (4) x 2
S(1)-K(1)	3.305 (3)	S(3)-K(2)	3.378 (2) x 2
S(1)-K(1)	3.299 (3)		
S(1)-K(2)	3.334 (4)	S(4)-In(2)	2.471 (2) x 2
S(1)-K(2)	3.422 (4)	S(4)-K(1)	3.274 (3) x 2
		S(4)-K(2)	3.379 (2) x 2
S(2)-In(1)	2.448 (2)		
S(2)-In(2)	2.447 (2)	S(5)-In(1)	2.439 (2)
S(2)-K(1)	3.188 (3)	S(5)-In(2)	2.438 (3)
S(2)-K(1)	3.992 (3)	S(5)-K(1)	3.174 (3)
S(2)-K(2)	3.977 (3)	S(5)-K(2)	3.183 (3)
S(2)-K(2)	3.194 (3)	S(5)-K(2)	3.997 (3)
		S(5)-K(2)	3.986 (3)

S(2)-In(1)-S(3)	109.5(1)	S(1)-In(2)-S(2)	108.9(1)
S(2)-In(1)-S(1)	107.8(1)	S(1)-In(2)-S(4)	111.2(1)
S(3)-In(1)-S(1)	109.1(1)	S(2)-In(2)-S(4)	107.8(1)
S(2)-In(1)-S(5)	105.1(1)	S(1)-In(2)-S(5)	110.9(1)
S(3)-In(1)-S(5)	111.8(1)	S(2)-In(2)-S(5)	105.3(1)
S(1)-In(1)-S(5)	113.3(1)	S(4)-In(2)-S(5)	112.5(1)

* Bond angles around the potassium atoms are included with the supplementary material.

FIGURE CAPTIONS

Figure 1. Representations of the $[In_4S_{10}]$ unit in $KInS_2$-I. (a) Ball-and-stick plot with 50% probability thermal ellipsoids emphasizing the adamantane-like structure; (b) polyhedral plot emphasizing the analogy to vapor-phase P_4O_{10}.

Figure 2. Perspective view of one layer of $KInS_2$-I approximately along (001) illustrating the interconnections of the $[In_4S_{10}]$ units and the channels of potassium atoms.

Figure 3. Polyhedral representation of the layers of vertex-linked $[In_4S_{10}]$ units in $KInS_2$-I. Each layer is rotated 90° relative to neighboring layers. The edges of the large $[In_4S_{10}]$ units in one layer nestle into the channels of the layers above and below, thus completing the trigonal prisms about the potassium atoms.

Figure 4. Views along the channels of potassium atoms showing the interlayer connections in $KInS_2$-I. (a) Ball-and-stick plot with 50% probability ellipsoids and with interatomic distances noted; (b) polyhedral plot.

Fig 1

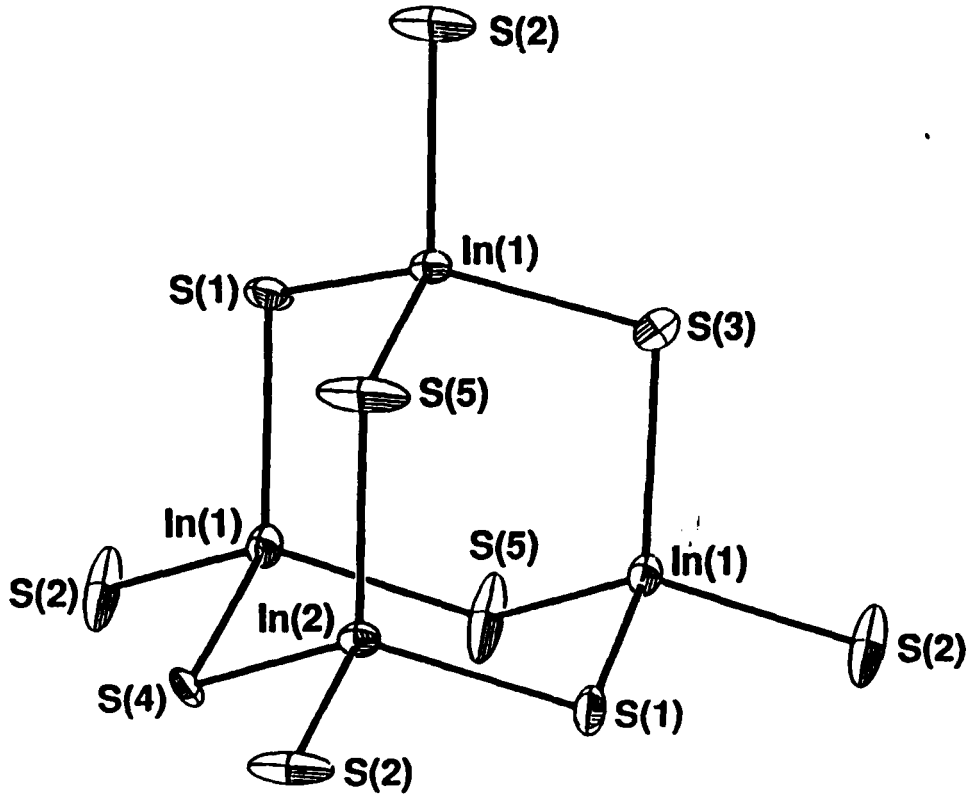

1a

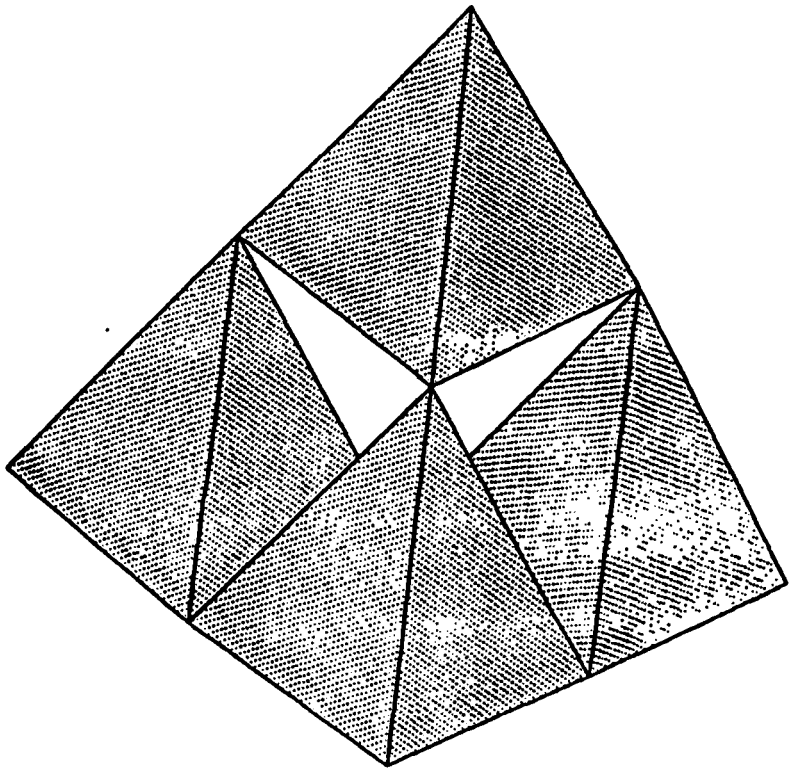

1b

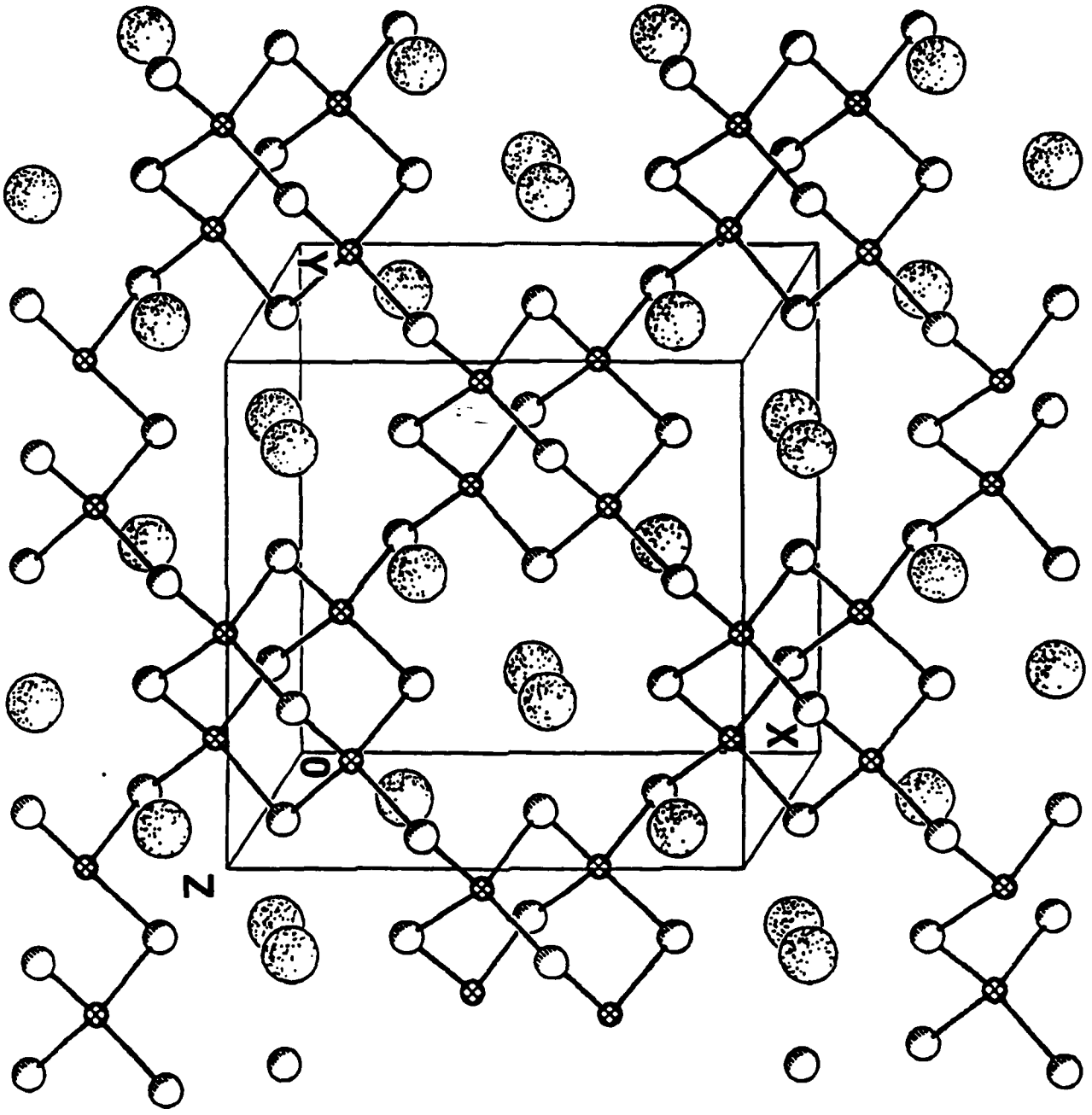

Fig. 6

Fig 3

Fig. 4

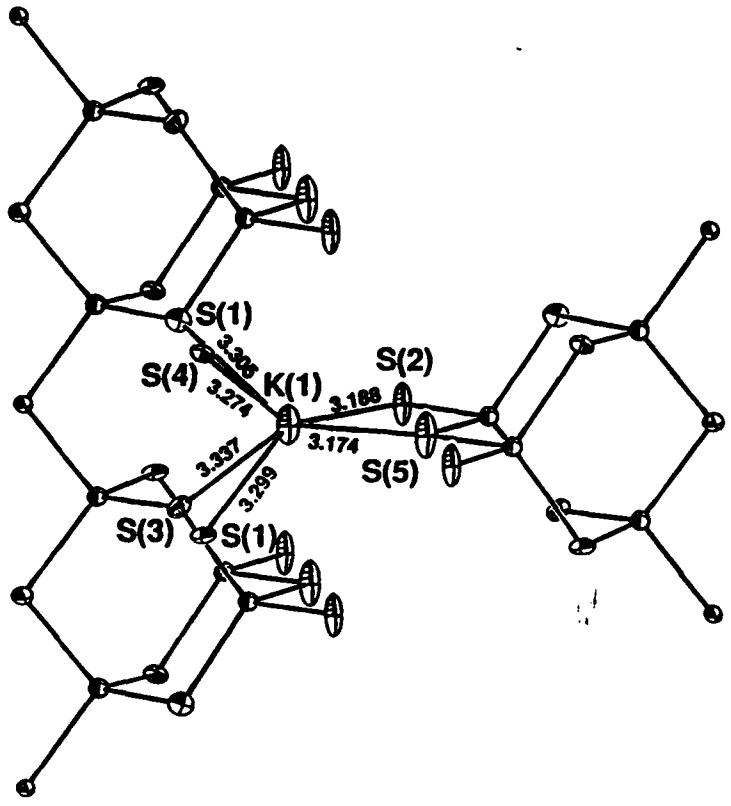

4a

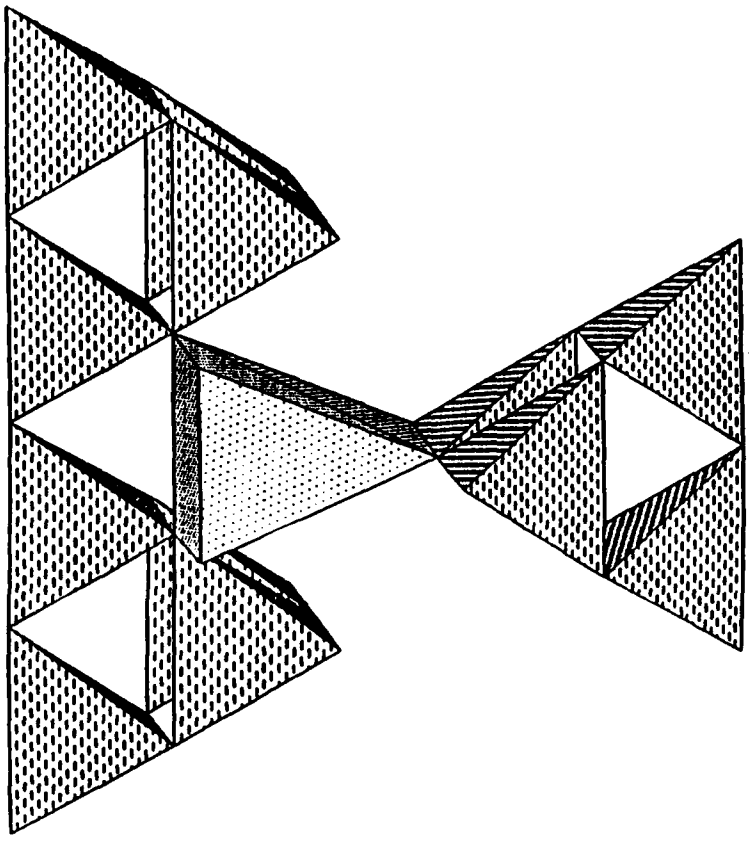

4b